Quick Computing Numerical Model of Pollutant Dispersion in Urban Street canyon

M. Biliaiev[1], T. Rusakova[2], V. Biliaieva[3], O. Berlov[4], V. Kozachyna[5], P. Kirichenko[6]

[1]*Ukrainian State University of Science and Technology, Lazaryan, 2, 49010, Dnipro, Ukraine,*
E-mail: biliaiev.m@gmail.com
[2]*Oles Honchar Dnipro National University, Haharin av. 72, 49010, Dnipro, Ukraine, E-mail: rusakovati1977@gmail.com*
[3]*Oles Honchar Dnipro National University, Haharin av. 72, 49010, Dnipro, Ukraine, E-mail: biliaiev.m@gmail.com*
[4]*Prydniprovska State Academy of Civil Engineering and Architecture, Chernyshevsky 24a, 490600, Dnipro, Ukraine,*
E-mail: berlovalexandrr@gmail.com
[5]*Ukrainian State University of Science and Technology Lazaryan 2, 49010, Dnipro, Ukraine,*
E-mail: v.kozachyna@gmail.com
[6]*Kryvyi Rih National Universitytate, Vitaliy Matusevych Street, 11, 50000, Kryvyi Rih, Ukraine,*
E-mail: pasha12922@gmail.com

Abstract

This research proposes a numerical model for the quick calculation of air pollution by emissions from cars in urban area such as "canyon". The Euler equations written in Helmholds variables were used to calculate the wind flow velocity field in street canyon. A special technique is used to calculate the vorticity in the corner points of buildings and barriers near the road. To calculate pollutant concentration field in the street canyon, which is formed from the traffic flow, the mass transfer equation was used, which took into account pollutant emission rate from cars, atmospheric diffusion, gravitational deposition, convective transfer. For numerical integration of modeling equations change-triangular finite-difference schemes were used The computer code realizing the developed numerical model was developed. The results of computational experiments to estimate the level of air pollution for different variants of the "canyon" scheme are presented.
KEY WORDS: *auto transport, air pollution, canyon, velocity field, pollution concentration level, difference methods*

1. Introduction

It is known that motor transport is the largest source of air pollution in cities. Road emissions cause an increased risk of asthma and other respiratory diseases. One proposed solution is to build barriers along busy roads to reduce roadside concentrations associated with road emissions [1-2]. For this reason, the interest to the formation of pollution zones on the streets during emissions from vehicles has increased significantly. An experimental study of the processes of atmospheric air pollution in the streets requires a significant amount of time to organize and conduct an experiment, both in laboratory and in natural conditions, and requires the use of expensive equipment. Therefore, to solve problems of this class, the method of mathematical modeling is actively used.

The method of mathematical modeling, empirical and semi-empirical models, Gaussian models, obtained on the basis of previous studies, are often used. These models can be used to assess the level of atmospheric air pollution near highways [2-4]. These models allow you to quickly calculate the concentration of the pollutant, but do not allow you to determine the pattern of concentration on the street where various objects are located. This does not allow using these models to study the issue of assessing various kinds of protective measures implemented to minimize the level of atmospheric air pollution near the road on the street. The most effective methods for studying the patterns of formation of pollution zones from vehicles on the streets is the use of CFD models. One of the important distinguishing features currently used in CFD models is the choice of fluid dynamics model. The most actively used models are those that use the Navier-Stokes equations to calculate the air flow velocity field in building conditions. The application of these equations is carried out using various turbulence models [5-8]. This models make it possible to study in detail the regularities of the formation of pollution zones in building conditions, but their application requires powerful computers and a fairly long time for calculations. Another approach in the field of mathematical modeling of atmospheric air pollution by emissions from vehicles is the use of a hydrodynamic model of a nonviscous fluid, in particular, a potential flow model [9]. This model allows within a few seconds to calculate the field of air pollution near the highway in the presence of various objects that affect the hydrodynamics of the flow near the route.

In this paper, a method has been developed for numerically calculating the field of air flow velocity and the concentration of atmospheric air pollution by emissions from cars in urban areas of the "canyon" type. Mathematical modeling was carried out using finite difference methods. A program has been created for carrying out computational experiments that do not require large expenditures of computer time. These studies may be useful in the design phase of the placement of barriers to reduce roadside emission concentrations.

2. Statement of the Problem and its Solution

2.1. Mathematical Model

A four-lane intra-city highway is considered, the width of one lane is 3.75 m. The considered computational area *ABCD* has the shape of a "canyon", since the residential area of multi-storey buildings is located on both sides of the road Fig. 1. Placing screens along the edge of the road is impractical, since this is a residential area and the entrance to the roadside must remain free on each side of the road. The task is to calculate the zone of atmospheric air pollution during the emission of SO_2 pollutants from vehicles, as well as to assess the effect of screens on reducing the value of the concentration of harmful substances in the residential area. A plane problem is being solved in the system of Cartesian coordinates *Oxy*: the *Ox* axis is directed horizontally, perpendicular to the movement of vehicles along the road (across the street), the *Oy* axis is directed vertically upwards.

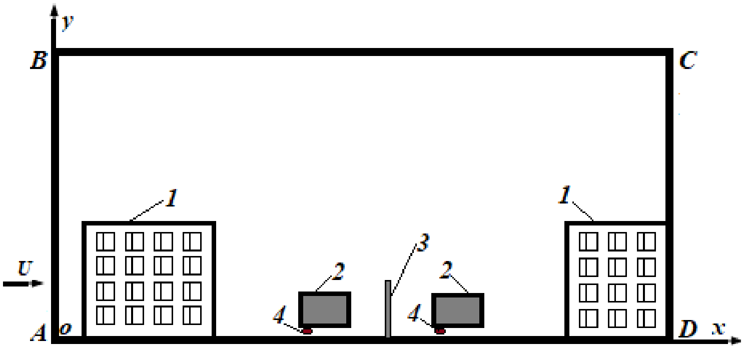

Fig. 1 The scheme: *1* – buildings; *2* – cars; *ABCD* – boundaries of the calculated domain; *3* – protective barrier (screen); *4* – emission source (car exhaust pipe)

In order to predict the level of pollution on the street during the emission of pollutants from vehicles, two problems need to be solved. The first problem is to determine the field of air flow velocity on the street, which is formed under the influence of buildings and cars on the movement of the air flow. The second task is to calculate the pollutant concentration field.

To solve the first problem, the Euler Eq. (1) is used, which is written in Helmholtz variables [11]:

$$\frac{\partial \omega}{\partial t}+u\frac{\partial \omega}{\partial x}+v\frac{\partial \omega}{\partial y}=0\,; \tag{1}$$

$$\frac{\partial^2\psi}{\partial x^2}+\frac{\partial^2\psi}{\partial y^2}=-\omega\,, \tag{2}$$

where ω – vortex; u, v – the components of the airflow velocity vector U; $\psi\,(x, y, t)$ – current function; x, y – Cartesian coordinates; t – time.

To calculate the flow hydrodynamics within this technique, it was assumed that the corner points inside the computational domain (the corner edges of buildings, cars) are sources of vortex generation. Therefore, to solve equations (1) – (2), the methodology for calculating the intensity of the vortex at the corner points was added using the Stokes theorem. The methodology is described in the work [11].

The values of the air flow velocity components are calculated after determining the current function according to the relations (3):

$$u=\frac{\partial\psi}{\partial y}\,;\ v=-\frac{\partial\psi}{\partial x}\,. \tag{3}$$

To solve modeling Eqs. (1) – (2), the following boundary and initial conditions must be met: at the boundary of the entrance to the computational domain *AB*: $\omega\big|_{AB}=\omega\big|_{entrance}$, in this case $\omega\big|_{entrance}=0$; $\psi\big|_{AB}=\psi\big|_{entrance}=\psi(y)$; $U\big|_{AB}=U\big|_{entrance}=U(y)$; on the upper boundary of the computational domain *BC*: $\frac{\partial\omega}{\partial\vec{n}}=0$, where $\vec{n}$ – the unit outward normal vector at the given boundary; $\psi=const$; on hard surfaces (surfaces of buildings, cars) that are impenetrable: $\frac{\partial\omega}{\partial\vec{n}}=0$; $\psi=const$; - at the edge of the air outlet *CD*: $\frac{\partial\omega}{\partial\vec{n}}=0$; $\frac{\partial\psi}{\partial\vec{n}}=0$; for the moment of time $t=0$

the initial condition is satisfied: $\omega|_{t=0} = 0$ – the absence of vorticity, which subsequently arises at the corner points of objects that are in the area.

To solve the second problem of calculating the pollutant concentration field, the mass transfer equation was solved. The previously calculated velocity field was the basis for solving the problem of pollutant mass transfer (4) [11].

$$\frac{\partial C}{\partial t}+\frac{\partial uC}{\partial x}+\frac{\partial vC}{\partial y}=\frac{\partial}{\partial x}\left(\mu_x\frac{\partial C}{\partial x}\right)+\frac{\partial}{\partial y}\left(\mu_y\frac{\partial C}{\partial y}\right)+\sum_{i=1}^{m}Q_i\delta(x-x_i)\delta(y-y_i)\,, \tag{4}$$

where $C(x,y,t)$ – concentration of pollutants CO, [kg/m^3]; u,v – components of the air flow velocity vector, [m/s]; μ_x, μ_y – diffusion coefficients, [m^2/s]; t – time, [s]; $Q_i(t)$ – emission intensity CO, [kg/(s·m^3)], x_i, y_i – coordinates of pollutant sources of emission sources, [m]; $\delta(x,y)$ – Dirac delta function; m – количество источников загрязнения. The Oy axis is directed vertically upwards; the Ox axis across the road (Fig. 1).

The diffusion coefficients are calculated by the formulas: $\mu_x = k_0 \cdot U$, $k_0 = (0{,}1 \div 1)$ m depending on the atmosphere stability level; U [m/s] – wind speed that is the known value of the wind flow velocity, can be calculated by the formula: $U = U_1 \cdot (y / y_1)^{n_1}$, where U_1 is the value of the wind speed at a certain fixed height y_1=3 m, $n_1 \approx 0.15 - 0.69$, since it depends on the roughness of the underlying surface and the stability class atmosphere, $n_1 = 0.15$ was taken in the work; $\mu_y = k_1\left(\frac{y}{y_1}\right)^{mm}$, $k_1 = (0{,}1 \div 0{,}2)$ m^2/s within the surface layer of the atmosphere [17], $mm \approx 1$.

To solve Eqs. (4) – (6), the following boundary conditions are set (Fig. 1): at the boundary *AB* the flow enters the computational domain, for the concentration of this impurity, a boundary condition $C|_{AB} = C|_{\text{entrance}}$ is set that is the background concentration, in the absence of data, the concentration value is taken to be zero; at the boundary *CD* the flow leaves the computational domain, at the end of the computational domain in the numerical model a boundary condition $\frac{\partial C}{\partial x} = 0$ is fulfilled, from a physical point of view, this condition means that the diffusion process at the flow exit boundary is not taken into account; at the boundaries *BC*, *AD* and on all solid walls, depending on the direction of the normal, the non-penetration condition must be satisfied.

2.2 Numerical Model

For the numerical solution of modeling Eqs. (1) – (3), a rectangular difference grid was used $(x,\ y)_{i,j} = (i \cdot \Delta x, j \cdot \Delta y)$, $i, j \in \text{integer}$. The solution of equation (1) by difference equations is carried out in two steps (5) – (6) [11].

In the first and the second splitting steps:

$$\frac{\omega_{i,j}^{n+1/2}-\omega_{i,j}^{n}}{\Delta t}+\frac{\overset{+}{u}_{i+1,j}\omega_{i,j}^{n+1/2}-\overset{+}{u}_{i+1,j}\omega_{i-1,j}^{n+1/2}}{\Delta x}+\frac{\overset{+}{v}_{i,j+1}\omega_{i,j}-\overset{+}{v}_{i,j-1}\omega_{i,j-1}}{\Delta y}=0\,; \tag{5}$$

$$\frac{\omega_{ij}^{n+1}-\omega_{ij}^{n+\frac{1}{2}}}{\Delta t}+\frac{\overset{-}{u}_{i+1,j}\omega_{i+1,j}^{n+1}-\overset{-}{u}_{i,j}\omega_{i,j}^{n+\frac{1}{2}}}{\Delta x}+\frac{\overset{-}{v}_{i,j+1}\omega_{i,j+1}^{n+1}-\overset{-}{v}_{i,j-1}\omega_{i,j}^{n+1}}{\Delta y}=0\,. \tag{6}$$

The unknown values of the vortex at each splitting step are determined from formulas (5) – (6) by relations (7) – (8):

$$\omega_{i,j}^{n+\frac{1}{2}}=\omega_{i,j}^{n}-\Delta t\frac{\overset{+}{u}_{i+1,j}\omega_{i,j}^{n+1/2}-\overset{+}{u}_{i+1,j}\omega_{i-1,j}^{n+1/2}}{\Delta x}-\Delta t\frac{\overset{+}{v}_{i,j+1}\omega_{i,j}-\overset{+}{v}_{i,j-1}\omega_{i,j-1}}{\Delta y}\,; \tag{7}$$

$$\omega_{ij}^{n+1}=\omega_{ij}^{n+\frac{1}{2}}-\Delta t\frac{\overset{-}{u}_{i+1,j}\omega_{i+1,j}^{n+1}-\overset{-}{u}_{i,j}\omega_{i,j}^{n+1}}{\Delta x}-\Delta t\frac{\overset{-}{v}_{i,j+1}\omega_{i,j+1}^{n+1}-\overset{-}{v}_{i,j-1}\omega_{i,j}^{n+1}}{\Delta y}\,. \tag{8}$$

The intensity of the vortex at the corner points, as noted above, is calculated according to [11].

For numerical integration of the Eq. (2) an explicit finite-difference scheme of numerical integration is used equation (9) reduces to an equation of the evolutionary type:

$$\frac{\partial\psi}{\partial\eta}=\frac{\partial^2\psi}{\partial^2 x}+\frac{\partial^2\psi}{\partial^2 y}+\omega\,, \tag{9}$$

where η is the dummy time, when $\eta \to \infty$, the solution of Eq. (9) goes to the solution Eq. (2). To solve this equation it is necessary to specify the initial condition at $\eta = 0$. For example, you can take $\psi_{\eta=0} = \psi_0$ to the entire calculation area. For numerical integration (9), an explicit difference scheme [10] is used, which has the form (10):

$$\psi_{i,j}^{n+1} = \psi_{i,j}^{n} + \Delta t \frac{\psi_{i+1,j}^{n} - 2\psi_{i,j}^{n} + \psi_{i-1,j}^{n}}{\Delta x^2} + \Delta t \frac{\psi_{i,j+1}^{n} - 2\psi_{i,j}^{n} + \psi_{i,j-1}^{n}}{\Delta y^2} + \omega_{i,j} . \quad (10)$$

The known values of the flow function $\psi_{i,j}^{n}$ make it possible to calculate the values of the components of the air flow velocity vector (11):

$$u_{i,j} = \frac{\psi_{i,j+1} - \psi_{i,j}}{\Delta y} ; \; v_{i,j} = -\frac{\psi_{i+1,j} - \psi_{i,j}}{\Delta x} . \quad (11)$$

For the numerical integration of equation (4), its physical splitting into the Eqs. (12) – (14):

$$\frac{\partial C}{\partial t} + \frac{\partial uC}{\partial x} + \frac{\partial vC}{\partial y} = 0 ; \quad (12)$$

$$\frac{\partial C}{\partial t} = \frac{\partial}{\partial x}\left(\mu_x \frac{\partial C}{\partial x} \right) + \frac{\partial}{\partial y}\left(\mu_y \frac{\partial C}{\partial y} \right); \quad (13)$$

$$\frac{\partial C}{\partial t} = \sum_{i=1}^{m} Q_i \delta\left(x - x_i\right) \delta\left(y - y_i\right) . \quad (14)$$

The following transformations were used to construct difference schemes (15) – (18):

$$\frac{\partial uC}{\partial x} = \frac{\partial u^+ C}{\partial x} + \frac{\partial u^- C}{\partial x} ; \; \frac{\partial vC}{\partial y} = \frac{\partial v^+ C}{\partial y} + \frac{\partial v^- C}{\partial y} ; \quad (15)$$

$$u^+ = \frac{u + |u|}{2} , \; u^- = \frac{u - |u|}{2} , \; v^+ = \frac{v + |v|}{2} , \; v^- = \frac{v - |v|}{2} ; \quad (16)$$

$$\frac{\partial u^+ C}{\partial x} \approx \frac{u_{i+1,j}^+ C_{i,j}^{n+1} - u_{i,j}^+ C_{i-1,j}^{n+1}}{\Delta x} = L_x^+ C^{n+1} ; \; \frac{\partial u^- C}{\partial x} \approx \frac{u_{i+1,j}^- C_{i+1,j}^{n+1} - u_{i,j}^- C_{i,j}^{n+1}}{\Delta x} = L_x^- C^{n+1} ; \quad (17)$$

$$\frac{\partial v^+ C}{\partial y} \approx \frac{v_{i,j+1}^+ {C^{n+1}}_{i,j} - v_{i,j}^+ {C^{n+1}}_{i,j-1}}{\Delta y} = L_y^+ C^{n+1} ; \; \frac{\partial v^- C}{\partial y} \approx \frac{v_{i,j+1}^- {C^{n+1}}_{i,j+1} - v_{i,j}^- {C^{n+1}}_{i,j}}{\Delta y} = L_y^- C^{n+1} . \quad (18)$$

The splitting scheme for Eq. (12) was performed in two steps (19) [11]:

$$\frac{C_{i,j}^{k} - C_{i,j}^{n}}{\Delta t} + {L^+}_x C^k + {L^+}_y C^k = 0 ; \; \frac{C_{i,j}^{n+1} - C_{i,j}^{k}}{\Delta t} + {L^-}_x C^{n+1} + {L^-}_y C^{n+1} = 0 . \quad (19)$$

For the numerical integration of Eq. (13), a two-stage difference splitting scheme was used (20) [11]:

$$\frac{C_{i,j}^{n+\frac{1}{2}} - C_{i,j}^{n}}{\Delta t} = \frac{-C_{i,j}^{n+\frac{1}{2}} + C_{i-1,j}^{n+\frac{1}{2}}}{\Delta x^2} + \frac{-C_{i,j}^{n+\frac{1}{2}} + C_{i,j-1}^{n+\frac{1}{2}}}{\Delta y^2} ; \; \frac{C_{i,j}^{n+1} - C_{i,j}^{n+\frac{1}{2}}}{\Delta t} = \frac{C_{i+1,j}^{n+1} - C_{i,j}^{n+1}}{\Delta x^2} + \frac{C_{i,j+1}^{n+1} - C_{i,j}^{n+1}}{\Delta y^2} . \quad (20)$$

For the numerical integration of Eq. (14), the Euler method was used (21) [10]:

$$C_{i,j}^{n+1} = C_{i,j}^{n} + \Delta t \cdot \sum_{i=1}^{m} Q_i \delta\left(x - x_i\right) \delta\left(y - y_i\right) . \quad (21)$$

To carry out computational experiments, a numerical calculation program "CANYON-2" was created in the FORTRAN programming language was developed.

2.4. Results of Computational Experiments

In this section, based on the developed method, the results of numerical calculation of the concentration field SO_2 from road transport emissions for three options for the location of the barrier in the canyon are presented. The first version of the calculation was carried out without a screen along the dividing strip of the road Fig. 2, the second - taking into account the presence of a screen with a height of H=5 m along the dividing strip Fig. 3, the third – taking into account the presence of a T-shaped screen with a height of H=5 m along the dividing strip (Fig. 4. The computational area Fig. 1 had dimensions: the length AD was 44 m, the height AB was 21.6 m. The emission intensity was 1 g/(s·m). At the AB boundary, the airflow velocity was 4 m/s, is the value of the wind speed at height 3 m. The Fig.2 – Fig.4 show the distribution of the concentration field as a percentage of the maximum value of the concentration $C_{\max}$. At the first stage of the study, based on the "CANYON-2" program, computational calculations were carried out in the study area without a protective barrier on the median strip (Fig. 2).

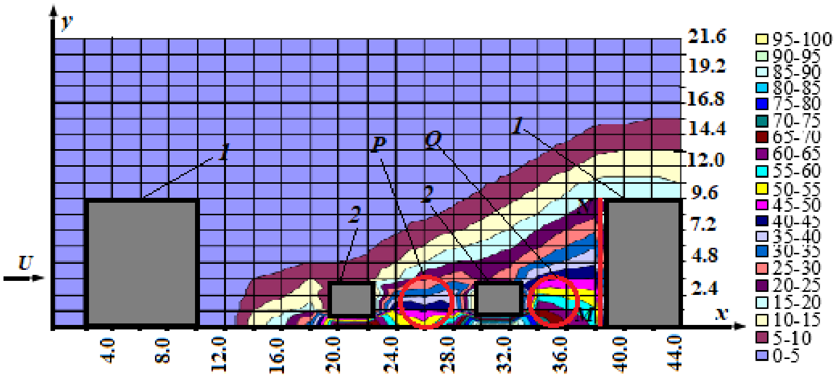

Fig. 2 Results of calculating the concentration field SO_2 in the absence of a barrier, C_{max} = 0,0272 mg/m^3: *1* – buildings; *2* – vehicles

The analysis of the results of calculations of the concentration field presented in Fig. 2 shows that zones P and Q are formed (highlighted by red circles) with an increased concentration value, which is 65-85% of the maximum value C_{max} = 0.0272 mg/m^3. The location of residential buildings according to the type of street canyon leads to the fact that the level of transport emissions at the height of the first and second floors (line MN) is about 51-56% of the maximum value on the road, so it is advisable to use technical methods to reduce the level of pollution concentration, namely protective barriers.

Therefore, at the second stage of the study, computational calculations were carried out in the study area in the presence of a protective barrier on the median strip (Fig. 3). The presence of a barrier in Fig. 3 contributes to the fact that at the location of the screen, the concentration line rises higher by 2.4 m, compared to Fig. 2. This suggests that the barrier acts as an obstacle, slowing down the movement of the polluted air flow. The decelerated flow moves upwards along the barrier, raising pollution to a greater height, where pollution is more effectively dissipated due to diffusion. The concentration value directly behind the barrier on the road (in zone P_2) becomes 20% lower than in zone P_1.

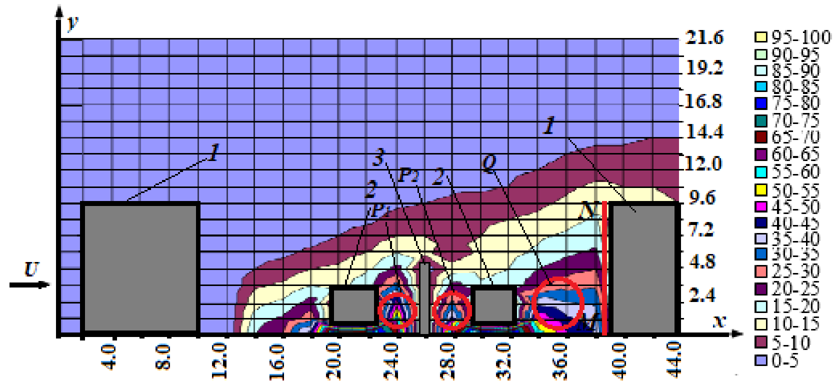

Fig. 3 The results of the calculation of the SO_2 concentration field taking into account the barrier H = 5 м, C_{max} = 0,0332 mg/m^3: *1* – buildings; *2* – vehicles; *3* – protective barrier (screen)

The location of the buildings in the form of a canyon creates additional obstacles for the moving polluted air flow. This is clearly seen in the shape of the lines of concentration, which are drawn in near the second building from its windward side. There are stagnant zones at the bottom of the building, from where pollution is poorly taken out. But since the polluted air rises to a greater height due to the screen, the level of concentration in the stagnant zones becomes less. In zone Q in Fig.3 the concentration level is reduced by 30% compared to the concentration level in zone Q in Fig. 2 where there was no barrier. At the height of the first and second floors near the second building (line MN), the concentration level is about 37-40% of the maximum value on the road $C_{max} = 0{,}0332$ mg/m^3. This confirms the effectiveness of a protective barrier on the median strip.

At the next stage of the study, computational calculations were carried out in the study area in the presence of a T-shaped protective barrier on the median strip Fig. 4. The Fig. 4 shows the distribution of SO_2 concentration in the case of using a T-screen. This form of the screen not only serves as an obstacle to the polluted air flow, but also directs it in opposite directions. Thus, the concentration level in zone Q_1 increases, and in zone Q_2 decreases. There is a forced equalization of the concentration of pollution in the zones Q_1 and Q_2. At the height of the first and second floors near the second building (line MN), the SO_2 concentration level is about 19 – 21% of the maximum value on the road $C_{max} = 0.05$ mg/m^3. The use of a protective T-shaped barrier on the median is more appropriate.

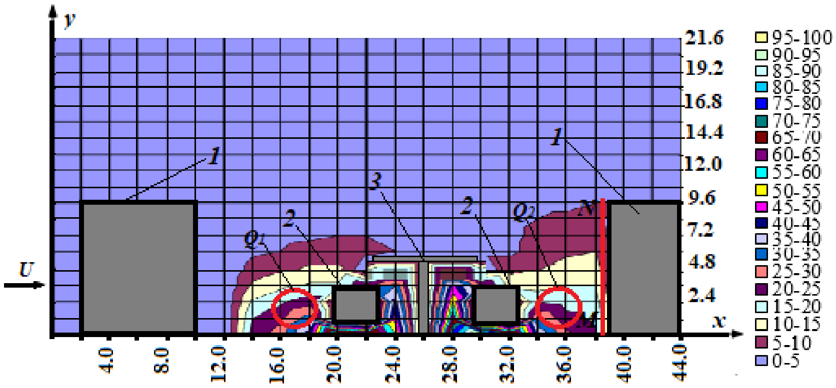

Fig. 4 The results of the calculation of the SO_2 concentration field taking into account the T-shaped barrier $H = 5$ м, C_{max}=0,05 mg/m^3: *1* – buildings; *2* – vehicles; *3* – protective T-shaped barrier (screen)

For a more detailed analysis of the results of numerical calculation in Fig. 2 – Fig. 4, a vertical section MN was chosen on the windward side of the second building. The relative reduction in concentration over the entire MN section when using a straight vertical screen was 20.7%, when using a T-shaped vertical screen was 41.8% when compared with the option of no screen.

In this study, on the basis of the developed method of numerical calculation, the tasks of using protective screens along the dividing strip of the road in the territory of street canyons were solved. The wide possibilities of using this method for numerical calculation of the concentration field of emissions from motor vehicles are shown, which is a necessary tool for carrying out measures for the reorganization of roads in the city.

3. Conclusions

An efficient numerical method is proposed for calculating the concentration field in urban areas like a street canyon, where highways with heavy traffic flow pass. This method makes it possible to take into account: the height of buildings, the geometric dimensions of vehicles and their position on the road, the presence of protective barriers of various heights and shapes, changes in the velocity field in the computational area of the canyon. Computational calculations were carried out on the basis of the developed program "CANYON-2", the calculation time was about 7 s.

The developed method can be used to establish transport logistics in the city, to justify the number of storeys of buildings during their new construction, to assess the level of air pollution from vehicle emissions in the urbanized areas of the city in order to ensure the environmental safety of the population.

References

1. **Belyaev, N.N.; Rusakova, T.I.; Kirichenko P.S.** 2014. Modeling of atmospheric air pollution by auto transport emissions on city streets, Dnepropetrovsk: Accent, 159 p.
2. **Bilyaev, M.M.; Rusakova, T.I.; Berlov O.V.** 2021. Minimization of the level of chemical pollution of the atmospheric wind on the surface, Dnipro: Zhurfond, 198 p.
3. **Schulte, N.; Venkatram A.** 2013. Effects of Sound Barriers on Dispersion from Roadways. DRAFT Final Report. Mechanical Engineering Bourns College of Engineering, 100 p.
4. **Sathe Yogesh, V.** 2012. Air Quality Modeling in Street Canyons of Kolhapur City, Universl Journal of Environmental Research and Technologies 2(2): 97-105.
5. **Shuo-Jun, Mei; Zhiwen, Luo; Fu-Yun, Zhao; Han-QingWang** 2019. Street canyon ventilation and airborne pollutant dispersion: 2-D versus 3-D CFD simulations, Sustainable Cities and Society 50: 101700.
6. **Zhong, Jian; Cai, Xiao-Ming; Bloss, William**. 2015. Modeling the Diospersion and Transpotrt of Reacrive

Pollutanys in Deep Urban Street Canyon, using large-eddy simulation, Environmental Pollution 200: 42-52.

7. **Pulvirenti, Beatrice et al.** 2020**.** Numerical Simulation of Air Pollution Mitigation by Means of Photocatalytic Coatings in real-world Street Canyons**,** Building and Environment 186: 1-13.
8. **Zhang, Y.; Yang, X.; Yang, H.; Zhang, K.; Wang, X.; Hang, J.; Luo, Z. and Zhou,** S. 2020. Numerical investigations of reactive pollutant dispersion and personal exposure in 3D urban-like models, Building and Environment, Vol. 169: 106569.
9. **Biliaiev, M.; Pshinko, O.; Rusakova, T.; Biliaieva, V.; Sladkowski, A.** 2021. Computer Model for Simulation of Pollutant Dispersion Near the Road with Solid Barriers. Transport Problems, Vol. 16, Issue 2, Part 1 : 73 -86.
10. **Samarsky, A.A.; Mikhailov, A.P.** 2001. Mathematical Modeling. Moscow: Fizmatlit, 320 p.
11. **Zgurovsky, M.Z.; Skopetsky, V.V.;Khrushch, V.K.; Biliaiv, M.M.** 1997. Numerical modeling of the spread of pollution in the environment, Kiev: Naukova dumka, 368 p.